

## Differential Endocytosis of CD4 in Lymphocytic and Nonlymphocytic Cells

By Annegret Pelchen-Matthews, Jane E. Armes, Gareth Griffiths,\* and Mark Marsh

From the Chester Beatty Laboratories, Institute of Cancer Research, London SW3 6JB, England; and the \*European Molecular Biology Laboratory, 6900 Heidelberg, Federal Republic of Germany

### Summary

The endocytosis of the T cell differentiation antigen CD4 has been investigated in CD4-transfected HeLa cells, the promyelocytic HL-60 cell line, and in a number of leukemia- or lymphoma-derived T cell lines. CD4 internalization was followed using radioiodinated antibodies in an acid-elution endocytosis assay, or by covalently modifying cell surface proteins with biotin and analyzing CD4 distributions by immunoprecipitation; both approaches gave equivalent results. The assays demonstrated that in transfected HeLa cells and in HL-60 cells CD4 was constitutively internalized and recycled in the absence of ligand. Immunogold labeling and electron microscopy demonstrated that CD4 enters cells through coated pits.

In contrast to the nonlymphocytic cells, T cell lines showed very little endocytosis of CD4. Measurements of fluid phase endocytosis and morphometric analysis of the endosome compartment indicated that the endocytic capacities of HeLa and lymphoid cells are equivalent and suggested that the low level of CD4 uptake in lymphocytic cells is due to exclusion of CD4 from coated pits. This conclusion was supported by experiments using truncated CD4 molecules, lacking the bulk of the cytoplasmic domain, which were internalized equally efficiently in both transfected lymphocytes and HeLa cells. Together, these results indicate that the cytoplasmic domain of CD4 mediates the different interactions with the endocytic apparatus in lymphoid and nonlymphoid cells. We suggest that the CD4-associated lymphocyte-specific protein tyrosine kinase p56<sup>lck</sup> may be involved in preventing CD4 endocytosis in T cells.

CD4, the T lymphocyte differentiation antigen (1, 2) and receptor for the human immunodeficiency viruses (HIV-1 and -2; reference 3), is expressed primarily on T cells restricted to the class II major histocompatibility complex (MHC-II)<sup>1</sup>, and on some cells of the macrophage/monocyte lineage (4). Although its function in the latter cells is not clear, CD4 is involved in thymocyte ontogeny and in the activation of peripheral T cells (5). In these events it appears to function in two ways. First, it increases the avidity of low affinity interactions between the TCR and MHC-II/antigen complexes by binding to nonpolymorphic regions on the MHC-II molecule (6, 7). Second, CD4 may have some intrinsic signalling capacity, as T cell stimulation through the TCR/CD3 complex can be inhibited by certain anti-CD4 monoclonal antibodies (8–10) and, in T cells, CD4 is found associated with the tyrosine kinase p56<sup>lck</sup> (11, 12).

For both MHC-II binding and signal transduction the functional site for the CD4 molecule appears to be at the plasma

membrane, and published data suggest that in T cells CD4 is only internalized after T cell activation or treatment with phorbol esters (13–15). These findings appear to conflict with our own observation that CD4 is constitutively internalized and recycled when expressed in CD4 cDNA-transfected HeLa and NIH-3T3 cells (16, 17), suggesting that either the interaction of CD4 with the endocytic pathway varies in different cell types, or that the antibody ligands we used to trace CD4 in HeLa cells induced internalization.

To clarify this issue, we have further characterized the endocytosis of CD4 in transfected HeLa cells and extended these studies to a number of leukemia- or lymphoma-derived T cell lines and the promyelocytic cell line HL-60. Here we show that in nonlymphoid cells cycling of CD4 occurs in the absence of ligand and involves coated pits. In contrast, CD4 is excluded from coated pits in lymphocytic cell lines and is not internalized efficiently. However, CD4 molecules from which the cytoplasmic domain has been deleted are internalized with equal efficiency in both transfected T cells and HeLa cells, indicating that the cytoplasmic domain of CD4 is involved in regulating CD4 endocytosis.

<sup>1</sup> Abbreviations used in this paper: BM, binding medium; HRP, horseradish peroxidase; MHC-II, class II major histocompatibility complex; Sv, surface to volume ratio; Vv, volume density.

## Materials and Methods

**Materials.** The anti-CD4 antibodies Leu3a (Becton Dickinson and Co., Mountain View, CA) and 4120 (provided by P. Beverley, Imperial Cancer Research Fund Human Tumour Immunology Group, University College, London, U.K.) compete for CD4 binding and appear to recognize the same or overlapping epitopes on the first V-like Ig domain of CD4. Both antibodies inhibit HIV gp120 binding to CD4 and behave identically in our endocytosis assays. The anti-CD4 antibody OKT4 (Ortho Diagnostic Systems, Raritan, NJ) binds to a distinct epitope on the third or fourth Ig-like domain of CD4. Antibodies and streptavidin were radiiodinated as described (16). Protein A-gold (9 nm) was prepared as described (18). Unless otherwise stated, all other reagents were from Sigma Chemical Co. (Poole, Dorset, U.K.).

**Cell Lines and Cell Culture.** HeLa cells and CD4-transfected derivatives (HeLa-CD4 and HeLa/CD4-cyt402; references 19, 20) were grown in DMEM supplemented with 4% FCS, 100 U/ml of penicillin and 0.1 mg/ml streptomycin, and used 3 d after subculture, when cell surface CD4 expression was maximal ( $\sim 2 \times 10^5$  and  $\sim 4 \times 10^5$  molecules per cell for HeLa-CD4 and HeLa/CD4-cyt402, respectively). The lymphocytic cell lines SupT1 (21) and CEM (22), as well as the CEM-derived A3.01, A2.01/CD4-cyt399, and A2.01/CD4-cyt401 lines (23) and the human promyelocytic leukemia cell line HL-60 (24) were grown in RPMI 1640 supplemented with 10% FCS, penicillin, and streptomycin as above, and used for experiments when they were growing exponentially. Under these conditions, SupT1 and CEM (or A3.01) cells expressed  $\sim 2 \times 10^5$  and  $\sim 8 \times 10^4$  cell surface CD4 molecules per cell, respectively, while the A2.01/CD4-cyt399 and A2.01/CD4-cyt401 cell lines had  $\sim 1.6 \times 10^5$ , and HL-60  $\sim 2.5 \times 10^4$  molecules of CD4 per cell. The CD4-transfected cell lines (HeLa/CD4-cyt402, A2.01/CD4-cyt399, and A2.01/CD4-cyt401) were grown in the presence of 0.4–1.0 mg/ml G418 (Gibco BRL, Paisley, Scotland).

**Production of Anti-CD4 Antiserum.** Antiserum to CD4 was produced by immunizing New Zealand White rabbits intradermally with 40  $\mu$ g recombinant soluble CD4 secreted from transfected CHO cells (reference 25; provided by Dr. R. Sweet of SmithKline Beecham Pharmaceuticals, King of Prussia, PA) in CFA and boosting at 2-wk intervals with 20  $\mu$ g soluble CD4 in IFA. The resulting serum contained antibodies that bound to soluble CD4 on Western blots, recognized CD4<sup>+</sup> but not CD4<sup>-</sup> cells by indirect immunofluorescence, competed with <sup>125</sup>I-Leu3a binding, and efficiently immunoprecipitated CD4 from SupT1 cells (26).

**Endocytosis Assay with <sup>125</sup>I-labeled Antibodies.** Internalization of CD4 in adherent cells was measured as described (16). For suspension cells the assay was adapted as follows. Cells were washed at 4°C with binding medium (BM; RPMI 1640 lacking bicarbonate, supplemented with 0.2% BSA and 10 mM Hepes, pH 7.4) and incubated with 0.3–1.5 nM <sup>125</sup>I-labeled Leu3a or 4120 antibody for 2 h at 4°C. Unbound <sup>125</sup>I-antibody was removed by washing three times by centrifugation (5 min at 1,500 rpm in an MSE Chillspin) and resuspension. The cells were then divided into two portions, one of which was kept over ice while the other was incubated at 37°C. After various times, duplicate aliquots of cells were withdrawn, cooled by dilution with ice-cold BM, and collected by centrifugation. To determine the proportion of internalized <sup>125</sup>I-antibody, cells from one aliquot per time point were suspended in low pH medium (cold BM adjusted to pH 2 with 10 mM morpholinoethanesulfonic acid and HCl) to remove cell surface ligand. The cells from the other aliquot were suspended in cold BM, pH 7.4. After incubating for 5 min on ice, triplicate aliquots of cells from each sample were collected by centrifugation through a cushion of 5% BSA in PBS. The supernatant and BSA cushion were re-

moved, and the amount of <sup>125</sup>I-antibody remaining in the cell pellets was measured by  $\gamma$ -counting.

**Cell Surface Biotinylation Endocytosis Assay.** HeLa and HeLa-CD4 cells were removed into suspension by incubating in 5 mM EDTA in PBS for 15 min at 37°C. Suspension cells were collected by centrifugation (5 min at 1,400 rpm in an MSE Chillspin). Cells were washed once in ice-cold PBS and suspended in freshly prepared 0.5 mg/ml N-hydroxysuccinimidyl-LC-biotin (NHS-LC-biotin; Pierce and Warriner, Chester, Cheshire, U.K.) in PBS at  $10^7$  cells/ml. After labeling for 30 min at 4°C with constant gentle agitation, cells were collected by centrifugation and washed twice in 0.2 M glycine in PBS. Cell viability was checked after labeling using trypan blue; usually >85% of the cells excluded the dye.

Surface-biotinylated cells were suspended in cold BM, divided into equal aliquots of  $2 \times 10^7$  cells and stored on ice or incubated at 37°C in a water bath. At various times, duplicate samples were cooled on ice and collected by centrifugation. From one of these samples, surface label was removed by suspending the cells in 0.15% bovine pancreatic trypsin (TPCK-treated) for 15 min at 4°C, and then washing twice in 2 mg/ml soya bean trypsin inhibitor in PBS. The resulting cell pellets were lysed at 4°C in 2% NP-40 (Pierce and Warriner) in 20 mM Tris-HCl, pH 8.0, containing 150 mM NaCl, 2 mM EDTA, and protease inhibitors (aprotinin, 6 U/ml; PMSF, 2 mM; antipain, 10  $\mu$ g/ml; chymostatin, 10  $\mu$ g/ml; leupeptin, 20  $\mu$ g/ml; and pepstatin A, 10  $\mu$ g/ml). Insoluble material was removed by centrifugation at 4°C at 10,000 g for 15 min. The post-nuclear supernatants were used directly or stored at  $-70^\circ\text{C}$ . Lysates were preabsorbed by incubation with 20  $\mu$ l of a nonspecific rabbit serum and cleared with  $2 \times 25 \mu$ l of packed protein A-sepharose CL-4B beads. For specific immunoprecipitation of CD4, lysates were incubated at ambient temperature ( $\sim 22^\circ\text{C}$ ) with 20  $\mu$ l rabbit anti-sCD4 serum for 1 h. Protein A-Sepharose beads (50  $\mu$ l packed volume) were then added and the incubation continued for 2 h (or overnight at 4°C) with constant agitation. Reprecipitation of lysates with anti-CD4 serum showed that this procedure consistently removed  $\sim 90\%$  of the CD4 present in the lysates (26). Beads with adsorbed CD4 were collected by centrifugation and washed by suspending twice in 0.3 M NaCl in 12.5 mM potassium phosphate buffer, pH 7.4, twice in mixed micelle buffer (10 mM Tris-HCl, pH 8.0, containing 0.3 M NaCl, 0.1% SDS, and 0.05% Triton X-100; Pierce and Warriner), and twice in distilled water. The precipitates were eluted with sample buffer, separated on 10% SDS polyacrylamide mini-gels, and transferred onto nitrocellulose (Schleicher and Schuell, Dassel, FRG). After quenching overnight in PBS containing 2% polyvinylpyrrolidone and 0.2% fatty acid-free BSA, blots were probed with <sup>125</sup>I-streptavidin and exposed to Kodak X-OMAT AR film for autoradiography. For quantitation, <sup>125</sup>I-streptavidin levels were determined by excising the labeled bands from the blots and  $\gamma$ -counting.

**Measurement of Fluid Phase Endocytosis.** Fluid phase endocytosis of HeLa-CD4 cells was measured using 5 mg/ml horseradish peroxidase (HRP, type II) in DMEM as described (27). Suspension cells (SupT1 and CEM) were collected by centrifugation, washed once in RPMI 1640, and suspended in pre-warmed or ice-cold medium containing 10 mg/ml HRP. At various times aliquots ( $\sim 10^7$  cells/point) were withdrawn and immediately diluted in cold BM. Cells were washed in the cold by suspension and centrifugation twice in BM, once in BM without BSA, and once in PBS. Viability was tested on one sample using trypan blue; usually, >95% of the cells excluded the dye. All remaining cell pellets were dissolved in PBS containing 0.5% Triton X-100. Levels of HRP in all cell lysates were determined using o-dianisidine in a microtitre plate assay essentially as described (28). Cell protein was

measured using bicinchoninic acid (Pierce and Warriner) as described (29).

**Electron Microscopic Localization of CD4.** For electron microscopy, HeLa, HeLa-CD4, or HeLa/CD4-cyt402 cells were seeded onto Thermanox plastic coverslips (Miles Scientific Div., Naperville, IL) and grown to confluence for 3 d. Lymphocytic cells were labeled in suspension. Cells were cooled and incubated on ice for 2 h with Leu3a or OKT4 (8 nM). Excess antibody was washed away, and the cells were labeled with protein A-gold. After 2 h, the cells were washed and either kept on ice or allowed to endocytose antibody-gold complexes at 37°C for various times. Cells were cooled by washing with ice-cold PBS and fixed on ice in 2.5% glutaraldehyde (BDH Ltd., Poole, Dorset, U.K.) in PBS. Cells were postfixated in osmium tetroxide, embedded in Epon, and thin sections were examined after staining with uranyl acetate and lead citrate.

**Measurement of Coated Pit Densities.** Densities of coated pits were measured on HeLa-CD4 cells harvested by incubation with 5 mM EDTA, or on exponentially growing CEM or SupT1 cells. Cells were fixed in 2.5% glutaraldehyde in 50 mM cacodylate buffer, pH 7.2, as described (30), to enhance the visibility of the clathrin coat. After embedding in Epon and sectioning, the ratio of coated pits to the total plasma membrane was estimated from the ratio of the number of intersections of a double-lattice grid (D64 from Weibel, reference 31) with coated pits to those over the whole plasma membrane (27).

**Morphometry of SupT1 Cells.** Two independent methods were used to determine the mean cell volume of fixed SupT1 cells. First, 1  $\mu$ m semi-thin sections of Epon-embedded SupT1 cells were prepared and random micrographs taken at a primary magnification of  $\times 1360$ . A grid of systematic test points was placed over the micrographs. For each point found over a cell, the intercept was measured with a ruler according to Gundersen and Jensen (32). This method makes no assumptions about cell shape, but since its predictions are volume weighted, it may overestimate the mean cell volume by as much as 10% (32, 33).

The second method assumes that the cells are spheres. Random electron micrographs of sections of Epon-embedded SupT1 cells were taken at a primary magnification of  $\times 952$  and enlarged to  $\times 3,895$ . The diameters ( $d$ ) of the cells were estimated using a ruler or a circular stencil. The diameters were classified into a histogram and corrected for underestimations of the smaller values (according to the method from Giger and Riedwyl, as described in reference 31). The mean diameter ( $D$ ) was then calculated using the formula:  $D = \pi/2Z$ , where  $Z = 1/N \sum n/d$  (34).  $N$  is the total number of profiles counted, and  $n$  is the number of profiles in each size class. The mean cell volume of HeLa-CD4 cells was determined using Method 2 of Griffiths et al. (33).

To measure the size of the endosome and lysosome compartments in SupT1 cells, exponentially growing cultures were harvested by centrifugation, washed once in warmed RPMI 1640, and incubated at 37°C in medium containing 10 mg/ml HRP type VI. The cells were incubated for 5 min or 4 h in order to selectively label the early endosomes or the whole endocytic pathway, respectively (27). Control cells were incubated with HRP medium at 4°C. The cells were then fixed, reacted with 0.1% diaminobenzidine and H<sub>2</sub>O<sub>2</sub> and embedded in Epon as described in reference 27. The volume density of the HRP-filled compartments was estimated stereologically by point counting as described (27). A double-lattice test grid (D64) was used, with the distance between the large test points = 60 mm (1.83  $\mu$ m at the magnification used) and that between the small test points = 5 mm (0.15  $\mu$ m).

To measure the volume density (Vv) of the nucleus and the sur-

face to volume ratio (Sv; references 27, 33) of SupT1 cells, micrographs were taken at a primary magnification of  $\times 2700$  and enlarged to a final magnification of  $\times 11,030$ . The Vv was estimated from point counting using a square lattice grid ( $d = 40$  mm;  $\approx 3.63$   $\mu$ m), while the Sv was calculated, using the same grid, by relating the number of intersections with the plasma membrane to the points falling on the cells.

## Results

**Endocytosis of Biotinylated CD4.** We have previously shown that the anti-CD4 monoclonal antibody Leu3a or its Fab' fragments are constitutively internalized and recycled in HeLa-CD4 cells (16). To examine whether CD4 is internalized and recycled in the absence of ligand, we developed an alternative endocytosis assay in which cell surface proteins on CD4<sup>+</sup> cells were covalently modified with biotin. CD4 was subsequently identified by immunoprecipitation with a specific anti-CD4 antiserum.

HeLa-CD4 cells were labeled using NHS-LC-biotin in PBS at 4°C, lysed in detergent and CD4 immunoprecipitated with a rabbit anti-CD4 antiserum. After SDS-PAGE, transfer to nitrocellulose and probing with <sup>125</sup>I-streptavidin, biotinylated CD4 was detected as a single band of  $\sim 54,000$  M<sub>r</sub>. This band was precipitated only from CD4<sup>+</sup> cells, but not from untransfected HeLa cells, and was not observed when lysates were precipitated with a nonspecific rabbit serum, or with anti-CD4 serum which had been preincubated with soluble CD4 (26). Furthermore, precipitation from biotinylated HeLa/CD4-cyt402 cells, which express a mutant form of CD4 from which the cytoplasmic domain has been deleted (see below), revealed a band with  $\sim 4$  kD lower molecular mass (not shown).

We investigated the ability of biotinylated CD4 to internalize during incubation of cells at 37°C. For this assay, HeLa-CD4 cells were removed into suspension by incubation with EDTA so that a large number of cells could be labeled in a small volume of NHS-LC-biotin solution in the cold. Control experiments demonstrated that the kinetics of <sup>125</sup>I-Leu3a uptake were the same when the cells were attached to plastic or in suspension (26). After biotinylation, cells were warmed to 37°C for various times to allow redistribution of labeled cell surface molecules, including CD4. To distinguish between internalized and cell surface CD4, cells were subsequently treated at 4°C with trypsin, which cleaves at several sites in the ectodomain of CD4 (35, 36). Cell lysates were prepared, and CD4 was immunoprecipitated and analyzed as described above.

Intact CD4 was readily precipitated from lysates of biotinylated HeLa-CD4 cells kept over ice, but could not be detected when the cells were treated with trypsin prior to lysis (Fig. 1 a, lanes 1 and 2). If biotin-labeled cells were warmed to 37°C for various times before trypsinization and lysis, a proportion of the CD4-biotin became trypsin resistant (lanes 4, 6 and 8) and must therefore have been internalized into a compartment protected from the externally applied protease. When the internalized material was quantitated by excising the <sup>125</sup>I-streptavidin-labeled bands from the blots

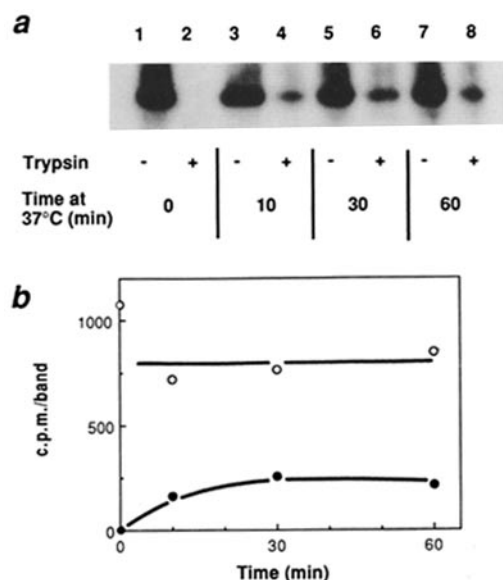


**Figure 1.** Endocytosis of biotin-labeled CD4 on HeLa-CD4 cells. (a) Autoradiogram of a CD4 immunoprecipitation blot probed with  $^{125}\text{I}$ -streptavidin. Surface-biotinylated HeLa-CD4 cells were kept on ice (lanes 1 and 2) or warmed to  $37^\circ\text{C}$  for 10 min (lanes 3 and 4), 30 min (lanes 5 and 6), or 60 min (lanes 7 and 8). Precipitates were prepared from lysates of these cells (lanes 1, 3, 5, and 7), or from cells that were trypsinized to remove surface CD4 prior to lysis (lanes 2, 4, 6, and 8). (b)  $^{125}\text{I}$ -streptavidin labeled bands were excised from the blot in a and bound radioactivity in total (lanes 1, 3, 5, and 7;  $\circ$ ) or trypsinized samples (lanes 2, 4, 6, and 8;  $\bullet$ ) estimated by  $\gamma$ -counting. In this experiment, the cells had been trace labeled with  $^{35}\text{S}$ -methionine to allow correction for differences in sample volumes, and for cell losses during the trypsinization step. When these corrections were applied, the plateau level of internalized (trypsin-resistant) CD4 at 30 and 60 min was 40% of the total cellular CD4-biotin.

and  $\gamma$ -counting, it was found that the amount of trypsin-resistant material increased to a plateau of  $\sim 40\%$  in 30–60 min (Fig. 1 b). This value is very similar to estimates of CD4 internalization obtained using  $^{125}\text{I}$ -Fab' fragments of Leu3a or  $^{125}\text{I}$ -Leu3a on attached HeLa-CD4 cells, thus confirming that the endocytosis of CD4 detected previously (16) occurs constitutively and independently of the presence of mono- or divalent ligand.

**Endocytosis of CD4 on Naturally CD4<sup>+</sup> Cell Lines.** The uptake of CD4 described above and previously (16) has been observed in transfected nonlymphoid cells. Since CD4 is normally expressed in lymphoid cells and on some cells of the macrophage/monocyte lineage, it was important to establish whether constitutive CD4 endocytosis and recycling also occurs on cells naturally expressing CD4. For these experiments we used an antibody-based endocytosis assay (16) in which cell surface CD4 is labeled in the cold with a soluble radioiodinated anti-CD4 monoclonal antibody. Antibody-labeled CD4 is then allowed to internalize by warming the cells to  $37^\circ\text{C}$ . Subsequently, the total cell-associated activity is measured or, alternatively, cell surface  $^{125}\text{I}$ -antibody is removed with an acid wash, leaving only internalized activity.

The result of a typical  $^{125}\text{I}$ -antibody endocytosis experiment with the promyelocytic cell line HL-60 is shown in Fig. 2. Endocytosis of CD4 could readily be demonstrated in these cells. CD4 was internalized at a rate of  $\sim 3\%$  per min, reaching a plateau with 40% of the initial cell surface CD4 in an intracellular compartment. Endocytosis of the  $^{125}\text{I}$ -labeled 4120 antibody was also observed when cells were labeled in the presence of a large excess of a nonspecific antibody of the same subclass as 4120, indicating that the uptake of  $^{125}\text{I}$ -antibody did not occur via Fc receptors. The pattern of CD4 endocytosis on HL-60 cells is very similar to that observed in CD4-transfected HeLa and NIH-3T3 cells (16, 17).

To analyze CD4 endocytosis in T cells we studied SupT1 cells, which express a high level of CD4 ( $\sim 10^5$  CD4 molecules/cell), and several other T lymphoma or leukemia lines. Endocytosis experiments with  $^{125}\text{I}$ -Leu3a revealed only a very low level of CD4 uptake in SupT1 cells (Fig. 3). When the level of acid-resistant  $^{125}\text{I}$ -Leu3a was calculated as a proportion of the total cell-associated activity (Fig. 3, inset), a small, but reproducible increase in acid-resistant activity could be observed. However, the steady-state level of acid-resistant activity was never  $>5$ – $8\%$  above the base level observed on cells which were kept at  $0$ – $4^\circ\text{C}$ . Similar results were obtained with CEM and MOLT-4 cells and, significantly, with an RPMI T cell line, which only expressed CD4 after transfection with the same CD4 construct used to generate the HeLa-CD4 cells (19).

Since the measurement of these low levels of internalization may be complicated by the dissociation of bound  $^{125}\text{I}$ -Leu3a from the cells, we also assayed CD4 endocytosis with the biotinylation/immunoprecipitation method (Fig. 4). As with the HeLa-CD4 cells, CD4-biotin on SupT1 cells was completely sensitive to trypsin treatment (Fig. 4 a, lane 2), but a trypsin-resistant band of internalized CD4-biotin appeared when the cells were warmed to  $37^\circ\text{C}$  (lanes 4, 6, 8, and 10). Quantitation by excising the bands from the blots and  $\gamma$

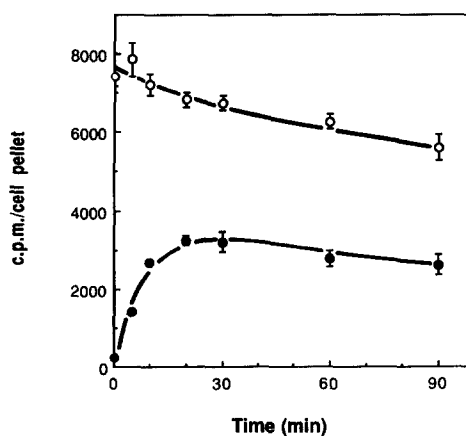


**Figure 2.** CD4 endocytosis on HL-60 cells. CD4 was traced on HL-60 cells using  $^{125}\text{I}$ -4120 antibody (0.6 nM). After warming  $^{125}\text{I}$ -4120-labeled cells for various times, levels of total cell-associated ( $\circ$ ) or low pH-resistant activity ( $\bullet$ ) were determined by acid washing and  $\gamma$ -counting. Error bars indicate standard deviations for measurements from triplicate cell samples.

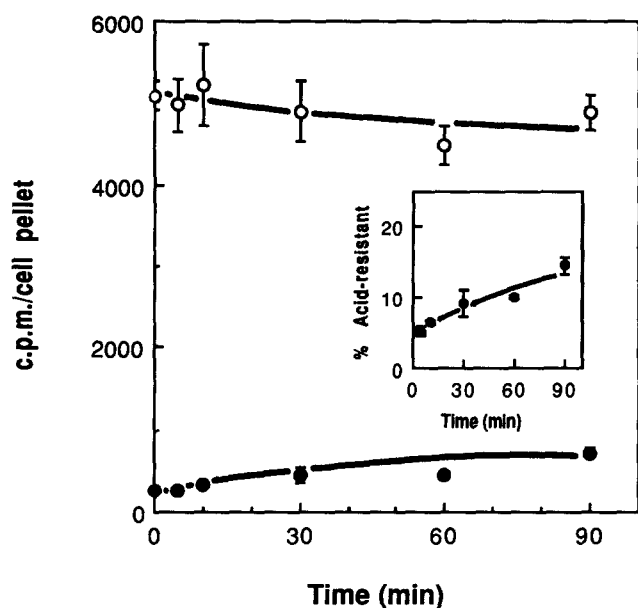


**Figure 3.** CD4 endocytosis on SupT1 cells. CD4 was traced on SupT1 cells using  $^{125}\text{I}$ -Leu3a antibody (0.3 nM). After warming labeled cells for various times, levels of total cell-associated (O) or low pH-resistant activity (●) were determined by acid washing. The inset shows the amount of acid-resistant activity as a proportion of the total. Error bars indicate standard deviations for measurements from triplicate cell samples.

counting (Fig. 4 *b*) revealed internalization to an equilibrium of between 5 and 10% of the initial cell surface CD4, corresponding closely to the levels of internalization detected with radioiodinated antibody. Low levels of CD4-biotin endocytosis could similarly be demonstrated on CEM and C8166 cells (not shown).

Thus, endocytosis of CD4 could be detected in a number of lymphocytic cell lines, but the levels of uptake were always five- to eightfold lower than those observed on HeLa-CD4 cells, suggesting that the endocytosis of CD4 differed between lymphoid and nonlymphoid cells. Although the reasons for these differences are unclear, two possibilities are that there may be differences in the endocytic capacities of the various cell types or in the interaction of CD4 with the endocytic apparatus. To distinguish between these possibilities, we first established the mechanism of CD4 internalization in HeLa-CD4 cells, and subsequently investigated the endocytic capacities of the various cell types.

**Electron Microscopic Localization of CD4 During Endocytosis in Transfected HeLa Cells.** Since CD4 is internalized constitutively in HeLa-CD4 cells in the presence or absence of ligand, we examined the route of uptake by electron microscopy. HeLa-CD4 cells were labeled on ice with Leu3a, excess antibody was washed away, and the cells were incubated with protein A-gold. After washing to remove the free gold conjugate, the cells were fixed and prepared for electron microscopy. Although only low densities of gold particles were observed (30–50 per HeLa-CD4 cell profile, which represents labeling of ~10% of the CD4 molecules), the labeling was specific,

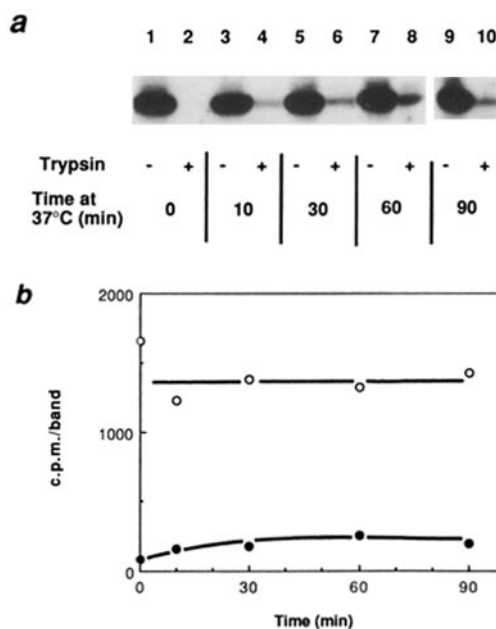


**Figure 4.** Endocytosis of biotin-labeled CD4 on SupT1 cells. (a) CD4 immunoprecipitation autoradiogram. Surface-biotinylated SupT1 cells were kept on ice (lanes 1 and 2) or warmed to 37°C for 10 min (lanes 3 and 4), 30 min (lanes 5 and 6), 60 min (lanes 7 and 8), or 90 min (lanes 9 and 10). Precipitates were prepared from lysates of these cells (lanes 1, 3, 5, 7, and 9), or from cells that were trypsinized to remove surface biotin label before lysis (lanes 2, 4, 6, 8, and 10). (b)  $^{125}\text{I}$ -streptavidin labeled bands were excised from the blot in *a* and bound radioactivity in the intact (O) or trypsinized samples (●) estimated by  $\gamma$ -counting.

since less than two particles per five cell profiles were observed on untransfected HeLa cells or on HeLa-CD4 cells incubated without the Leu3a antibody. Examination of the distribution of the gold particles revealed labeling of the plasma membrane and microvilli, with occasional particles in coated pits (Fig. 5 *a*). When the distribution was analyzed quantitatively, by examining cell surfaces and noting the location of every gold particle encountered (Table 1), 4.5% of the particles were adjacent to clathrin-coated areas of the plasma membrane. Since this pattern of labeling was observed on cells which were cooled before the addition of Leu3a and kept on ice throughout the incubation, it presumably reflects the steady state distribution of CD4 on the cell surface.

Internalization of CD4 was studied morphologically by warming cells which had been labeled as described above to 37°C for various times, and then fixing and processing for electron microscopy. Control experiments in which the kinetics of  $^{125}\text{I}$ -Leu3a uptake were examined after incubation with protein A-gold showed that internalization of the antibody was not affected by the gold probe (data not shown). When cells were warmed for 2 min, the distribution of gold particles observed at the cell surface was essentially identical to that on cells kept over ice, except that some particles were found in coated vesicles (Fig. 5 *b*). In addition, some gold particles were observed in intracellular smooth vesicular structures. By 5 min, 15% of the gold particles had been internalized into endosomal tubulo-cisternal structures, while after

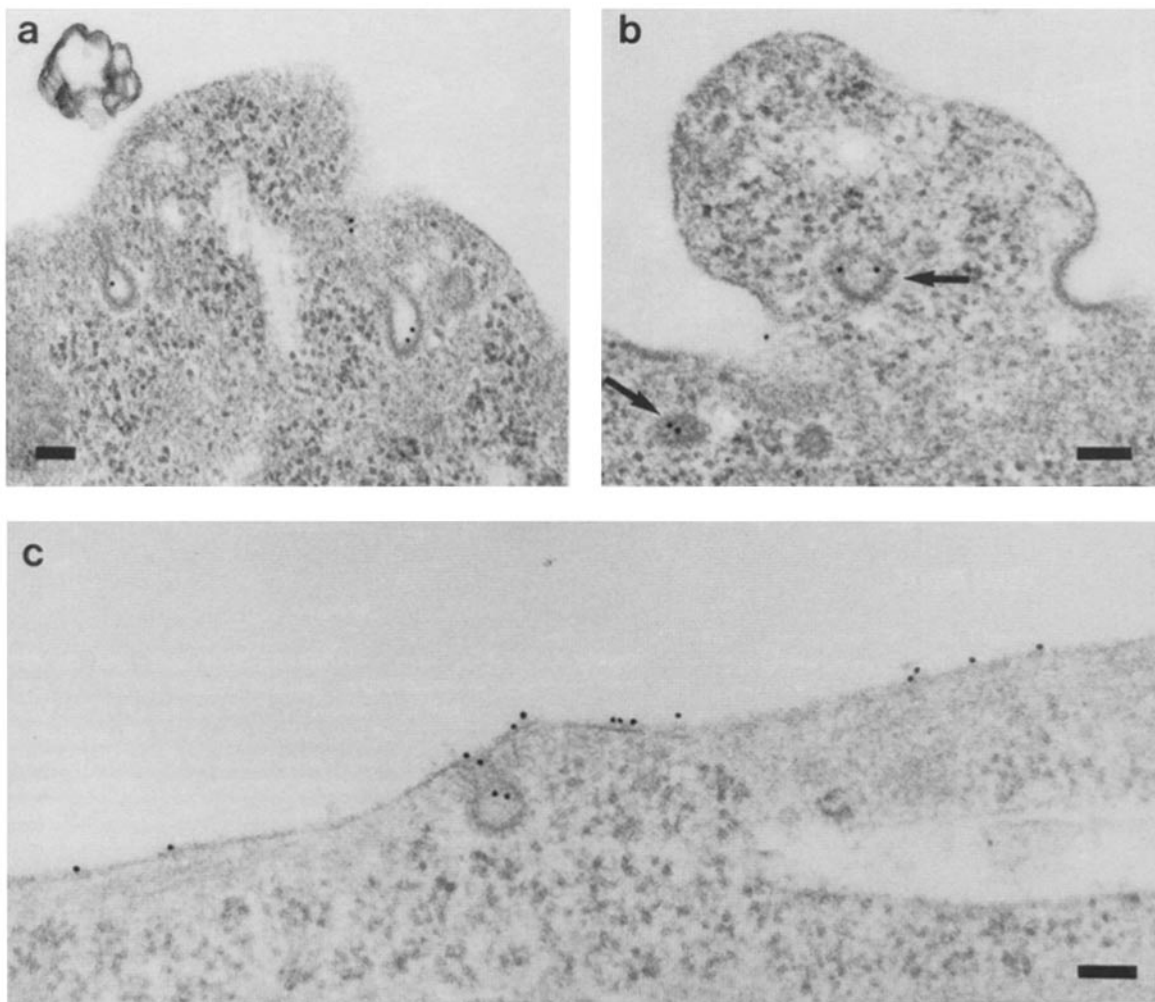


**Figure 5.** Electron microscope localization of CD4 on HeLa-CD4 (*a* and *b*) and HeLa/CD4-cyt402 cells (*c*). Cells were labeled on ice with 8 nM Leu3a (*a* and *b*) or OKT4 (*c*) followed by protein A-gold as described in Materials and Methods. Gold particles identify CD4 in coated pits (*a* and *c*) or coated vesicles (*b* arrows). Scale bars = 100 nm.

**Table 1.** Distribution of Gold-labeled CD4 on HeLa-CD4 Cells

Time at 37°C	Total no. of particles counted	Particles over noncoated plasma membrane		Particles over pits/vesicles*		Internalized particles		Unclassified
			%		%		%	
<i>min</i>			%		%		%	
0	530	499	(94.2)	24	(4.5)	0	(0.0)	7
2	417	363	(87.1)	19	(4.6)	18	(4.3)	17
5	263	207	(78.7)	6	(2.3)	39	(14.8)	11
30	405	220	(54.3)	0	(0.0)	185	(45.7)	0

Distributions of Leu3a/protein A-gold particles were analyzed as detailed in the text.

\* Only particles observed immediately adjacent to the clathrin coat were counted in this category. Particles close to the entrance of deep invaginations but not adjacent to the clathrin lattice (e.g., the two particles in Fig. 5 *c*) were counted as noncoated plasma membrane.

30 min, 48% of all gold particles were found inside the cells. This level of intracellular gold labeling is similar to the amounts of CD4 internalized in biochemical experiments (compare with reference 16 and above). After 5–30 min at 37°C there was a decrease in the proportion of gold particles observed in coated pits. Experiments using  $^{125}\text{I}$ -labeled antibody, together with detection of protein A–gold by silver enhancement suggest that this is a consequence of the dissociation of the protein A–gold reagent and does not reflect depletion of CD4 from coated pits.

The electron microscopy experiments thus confirm that CD4 is internalized in the transfected HeLa cells, and indicate that this internalization involves coated pits. If the half-life of a coated pit at the cell surface is assumed to be  $\sim 1$ –2 min (27, 37, 38), and the amount of CD4 observed in coated pits is 4.5% of the cell surface pool, then coated vesicles can account for all of the CD4 endocytosis (2% per min; see also reference 16) observed in HeLa-CD4 cells.

While the low densities of CD4 on HL-60 cells precluded similar analysis, electron microscopy was used to examine CD4 distributions on the lymphocytic cell lines SupT1 and CEM. In agreement with the low levels of CD4 uptake in these cells (see above), Leu3a/protein A–gold complexes were observed very infrequently in coated pit structures. Less than 0.6% of all gold particles counted were found in coated pits, and a complete quantitative analysis was not practicable.

**Quantitative Analysis of the Endocytic Capacity in Lymphocytes.** To determine the endocytic capacity of the different cell types, we measured fluid phase endocytosis in SupT1, CEM, and HeLa-CD4 cells using HRP (27, 39). As previously described for other cell types (27, 40, 41), fluid phase uptake of HRP showed curvilinear kinetics. Analysis of the rates of fluid phase endocytosis at early times (up to 10 min), when recycling is negligible and uptake linear, revealed that the lymphocytic cell lines internalized about half as much fluid per microgram cell protein as the HeLa-CD4 cells (Table 2). When calculated on a per cell basis, HeLa-CD4 cells accumulated  $\sim 15$  times as much HRP as the SupT1 and CEM cells. However, the HeLa-CD4 cells are much larger than the lymphocytic cells: Morphometric analysis indicated that the mean cell volumes of fixed and plastic-embedded SupT1 and HeLa-CD4 cells were 490 and 3,160  $\mu\text{m}^3$ , respectively.

**Table 2.** Fluid Phase Endocytosis of HRP

Cell line	Initial rate*	
	Protein nl/h/ $\mu\text{g}$	Cells nl/min/ $10^6$
SupT1	0.023 $\pm$ 0.008	0.028 $\pm$ 0.009
CEM	0.024 $\pm$ 0.004	0.038 $\pm$ 0.007
HeLa-CD4	0.049 $\pm$ 0.004	0.493 $\pm$ 0.036

\* Rates were measured over the first 10 min of the assay.

Similar volume estimates were made on live cells using 3-O-Methyl-D[1- $^3\text{H}$ ]glucose (42) or a channelizer (Coulter Electronics, Inc., Hialeah, FL), and together indicated that the volume of lymphocytic cells is three- to sixfold less than that of the HeLa cells. The rate of fluid phase endocytosis per unit cell volume is therefore at most two- to threefold greater in HeLa-CD4 cells than in lymphocytes and would not explain the five- to eightfold higher levels of CD4 endocytosis in the HeLa-CD4 cells.

As our previous studies have suggested that the majority of fluid phase endocytosis occurs through coated pits and coated vesicles (27, 38), and the results presented here indicate that CD4 is internalized via coated vesicles, we also measured coated pit densities for the three different cell types. This revealed that the proportion of the plasma membrane which had clathrin coats was 1.57, 1.59, and 1.18% on SupT1, CEM, and HeLa-CD4 cells, respectively. Thus, the proportion of coated membrane was comparable between the lymphocytic and the HeLa-CD4 cells. Coated pit densities of 1–2% have also been reported for a variety of other cell lines (27, 37, 43).

In addition to the rates of vesicle formation, the relative sizes of the endocytic compartments in lymphoid and HeLa cells may also influence endocytosis measurements. The CD4 endocytosis assays described above rely on the appearance of an intracellular acid- or trypsin-resistant pool of tracer. Thus a proportionally smaller endosome compartment in lymphocytes could account for an apparent lower level of CD4 endocytosis. Since immunofluorescence and electron microscopic localization, and preliminary cell fractionation experiments suggest that CD4 is internalized into endosomes (our un-

**Table 3.** Summary of Membrane Surface Areas and Volumes in SupT1 and BHK Cells

	SupT1	BHK
Cell volume ( $\mu\text{m}^3$ )	490 $\pm$ 44	1,400
Cytoplasm volume ( $\mu\text{m}^3$ )	229 $\pm$ 27	1,050
Plasma membrane SA ( $\mu\text{m}^2$ )	326 $\pm$ 37	2,200
Percent of plasma membrane coated	1.57 $\pm$ 1.4	1.6
Endosome volume/cytoplasm volume (%)	0.63	0.66
Lysosome + PLC* volume/cytoplasm volume (%)	1.58	3.52
Endosome SA/plasma membrane SA (%)	15.5	19.5
Lysosome + PLC* SA/plasma membrane SA (%)	42.2	16.8

Endosome and lysosome estimates were based on HRP labeling for 5 min (endosome) or 4 h (endosomes + lysosomes), respectively. Data for BHK cells were from Griffiths et al. (27).

\* Pre-lysosomal compartment (27).

published results), we measured the size of the endosome and lysosome compartments in one of the lymphocytic cell lines. SupT1 cells were incubated for 5 min or 4 h in medium containing HRP. Under these conditions, the label is either restricted to endosomes, or penetrates the entire endocytic pathway, respectively (27). The compartment sizes were then measured using established morphometric methods, and compared to the values previously derived for BHK-21 cells (27, 33). The results of this analysis (Table 3) indicated that the volume of the endosome compartment represented a similar proportion of the cytoplasmic volume in both SupT1 and BHK cells. Furthermore, the surface area of the endosome compartment was 16 and 20% of the surface area of the plasma membrane in the two cell types, respectively. While HeLa-CD4 cells were not directly evaluated in this analysis, similar numbers have been derived for several other cell lines, including NRK and MDCK (44, 45), suggesting that endosomal dimensions are very similar in a variety of cell types.

Collectively the fluid phase endocytosis measurements and morphometric analysis indicated that the endocytic capacities of HeLa-CD4 and lymphoid cells are very similar and do not explain the very different levels of CD4 endocytosis. The low levels of CD4 endocytosis observed in the lymphocytic cell lines may instead reflect differences in the ability of CD4 to interact with the endocytic coated pits in the different cell types.

**Internalization of Cytoplasmic-deleted CD4 Molecules.** CD4 is an integral membrane glycoprotein and contains a cytoplasmic domain of 38 amino acids (46). We investigated the role of the cytoplasmic domain in CD4 endocytosis using several transfected cell lines. HeLa/CD4-cyt402 cells (20) have been transfected with a mutant form of CD4, which lacks the bulk of the cytoplasmic domain (amino acids 403–433), leaving only seven cytoplasmic amino acids. In addition, we have used derivatives of the CEM cell line, A2.01, which do not express wild-type CD4 (47), but have been transfected with mutant forms of CD4 lacking 32 or 34 cytoplasmic amino acids (A2.01/CD4-cyt401 and A2.01/CD4-cyt399, respectively; reference 23).

When endocytosis was measured on HeLa/CD4-cyt402 cells using  $^{125}\text{I}$ -Leu3a (Fig. 6 a), a time-dependent increase in the level of acid-resistant tracer was observed, which reached a plateau after ~60 min. Thus, as with wild type CD4, the transfected CD4-cyt402 mutant was internalized in HeLa cells. Furthermore, while the rate of internalization (1%/min) and the steady-state levels of internalized CD4-cyt402 ( $17 \pm 3\%$  of total cell associated label,  $n = 3$ ) were about half those observed on HeLa-CD4 cells (16), they were significantly greater than those of SupT1 cells (above). As with intact CD4, the plateau of internalized CD4-cyt402 was due to recycling of the internalized CD4 (data not shown). Endocytosis of  $^{125}\text{I}$ -Leu3a on HeLa/CD4-cyt402 cells was not induced by the bivalent antibody tracer, since it was also observed when these cells were surface biotinylated and CD4 endocytosis measured after warming, trypsinizing, and immunoprecipitating as described above (Fig. 6 b).

The route of internalization of the cytoplasmic deleted molecules was studied by electron microscopy by labeling HeLa/

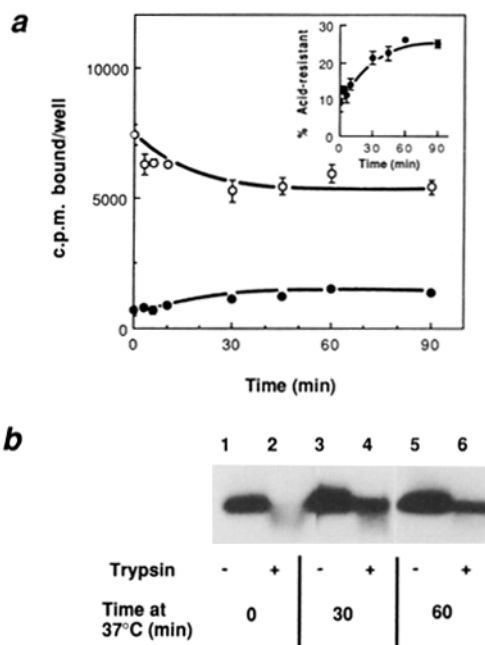


**Figure 6.** (a) Internalization of cytoplasmic-deleted CD4 on HeLa/CD4-cyt402 cells. HeLa/CD4-cyt402 cells were labeled with 0.36 nM  $^{125}\text{I}$ -Leu3a on ice, washed, and warmed to 37°C for various times. Levels of total cell-associated antibody (O) or acid-resistant antibody (●) were then determined by acid washing and  $\gamma$  counting. The inset shows the low pH-resistant activity as a proportion of the total. Error bars indicate SDs for measurements from three culture wells. (b) Endocytosis of biotinylated CD4-cyt402. CD4 was immunoprecipitated from surface-biotinylated HeLa/CD4-cyt402 cells kept on ice (lanes 1 and 2) or warmed to 37°C for 30 min (lanes 3 and 4) or 60 min (lanes 5 and 6). Precipitates were prepared from lysates of these cells (lanes 1, 3, and 5), or from cells that were trypsinized to remove surface biotin label before lysis (lanes 2, 4, and 6).

CD4-cyt402 at 0–4°C with the monoclonal antibody OKT4 and protein A–gold. HeLa/CD4-cyt402 cells express two to three times more CD4 per cell than HeLa-CD4 cells (data not shown), and were found to be very prominently labeled with protein A–gold (150–200 particles per cell profile). Quantitative analysis of the distribution of the gold particles indicated that in cells kept over ice, 1,174 out of 1,190 gold particles counted (98.7%) were on the plasma membrane and microvilli. In addition, 14 gold particles (1.2%) were seen adjacent to coated areas of the plasma membrane (Fig. 5 c). This density of CD4-cyt402 in coated pits corresponds closely with the proportion of coated plasma membrane in HeLa cells (compare with above), suggesting that the tailless CD4 is not concentrated in coated pits but enters cells passively as part of the bulk membrane flow. The reduced proportion of CD4-cyt402 in coated pits, compared to wild-type CD4 (compare with Table 1), is in agreement with the different rates of uptake of the two molecules measured biochemically (16).

Since HeLa/CD4-cyt402 cells internalized the mutant CD4 and, significantly, had higher levels of CD4 endocytosis than lymphocytic cells, it was important to examine the internalization of truncated CD4 molecules in transfected lymphocytic cell lines. Analysis of CD4 trafficking using the  $^{125}\text{I}$ -

antibody endocytosis assay on the A2.01/CD4-cyt399 and A2.01/CD4-cyt401 cells showed that tailless CD4 molecules were also internalized (Fig. 7). The truncated CD4 molecules were taken up at a rate of 1–1.3%/min, reaching steady state with 28 and 21% CD4 inside the A2.01/CD4-cyt399 and A2.01/CD4-cyt401 cells, respectively. These figures are very similar to the levels of tailless CD4 internalization in HeLa/CD4-cyt402 cells. By contrast, the A3.01 cell line, from which A2.01 cells were derived (47) and which expresses wild type CD4 (23), showed very low levels of CD4 endocytosis, similar to those observed in SupT1 cells (Fig. 7 *b*).

The distribution of CD4 on the A2.01/CD4-cyt401 cells was also studied by electron microscopy. After labeling with Leu3a and protein A gold, the A2.01/CD4-cyt401 cells contained ~20 gold particles per cell profile. As with the HeLa/CD4-cyt402 cells, quantitative analysis of the distribution of the gold particles showed that 16 out of 1,078 gold particles counted (1.5%) were adjacent to coated areas of the plasma membrane. Again, this density of truncated CD4 molecules in coated pits corresponds with the proportion of coated plasma membrane.

Thus both lymphoid and nonlymphoid cells internalized tailless CD4 molecules to similar levels, confirming that the endocytic capacities of these cells are similar. Furthermore,

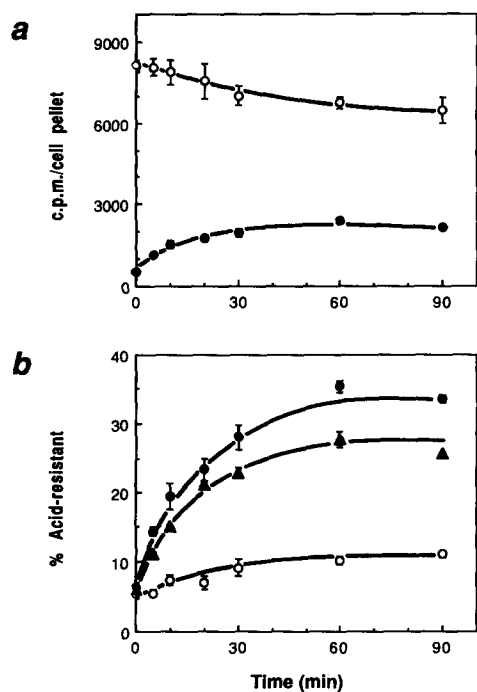


**Figure 7.** Endocytosis of cytoplasmic-deleted CD4 on lymphocytic cell lines (*a*) CEM-derived A2.01/CD4-cyt399 cells were labeled with  $^{125}\text{I}$ -4120 antibody (1.3 nM) in the cold. After warming the labeled cells for various times, the levels of total cell-associated antibody (O) or low pH resistant antibody (●) were determined by acid washing. (*b*) The amount of acid-resistant activity as a proportion of the total is shown for the A2.01/CD4-cyt399 cells (*a*, ●), as well as for A2.01/CD4-cyt401 cells (▲) and A3.01 cells, which express wild-type CD4 (O). Error bars indicate SDs for measurements from triplicate cell samples.

these results indicate that the cytoplasmic domain of CD4 is involved in permitting or preventing CD4 internalization in nonlymphoid and lymphoid cells, respectively.

## Discussion

In this paper we have shown that the T cell differentiation antigen CD4, when transfected into HeLa cells or naturally expressed in HL-60 cells, is constitutively endocytosed and recycled both in the presence and absence of antibody ligands. While the rates of internalization observed were lower than those of rapidly endocytosed molecules such as the receptors for low density lipoprotein (48) or transferrin (49), a significant proportion (~40%) of the CD4 was located in an endosomal compartment at steady state. In contrast, CD4 endocytosis in several lymphocytic cell lines was very inefficient, since only 5–10% of the CD4 was internalized in assays using either  $^{125}\text{I}$ -antibody or biotin labeling. The difference between the lymphoid and nonlymphoid cells was not due to the nature of the transfected CD4 in HeLa cells, since CD4 expressed from the same vector in a CD4 negative T cell line (RPMI 1640; reference 19) exhibited properties similar to those of CD4 normally expressed in lymphocytic cells.

To understand this difference in the endocytic properties of CD4, we examined the mechanism of CD4 internalization. Electron microscopic analysis of the CD4 distribution on HeLa-CD4 cells indicated that ~4.5% of the CD4-immunogold complexes were adjacent to clathrin-coated areas of the plasma membrane. As coated pits accounted for ~1.2% of the total plasma membrane area in these cells, this result suggests that the cytoplasmic domain of CD4 may interact with endocytic coated vesicle adaptors (50) and be enriched in coated pits. Furthermore, based on the estimated cell surface residence times of coated pits (1–2 min; references 27, 37, 38), our data indicate that coated vesicles can account for all of the CD4 endocytosis measured in transfected HeLa cells.

Similar analysis of the lymphocytic cells indicated that the proportion of CD4 associated with coated pits was significantly lower than that observed in HeLa cells and suggested that the low level of CD4 endocytosis observed in lymphoid cells is due to the exclusion of CD4 from coated pits. This conclusion was supported by three further observations. First, morphometric and fluid phase endocytosis measurements of SupT1 cells indicated that the relative endocytic capacities of the lymphoid cells and nonlymphoid cells were similar. Second, measurements of transferrin endocytosis indicated that the coated vesicle pathway was functionally active in the lymphoid cells (data not shown). Third, cytoplasmic-deleted mutant CD4 molecules were internalized to a similar extent in both transfected HeLa and lymphoid cells.

How can CD4 be excluded from coated pits on the lymphoid cells? Lymphocytes and HeLa cells may have different coated vesicle adaptors (50); however, since the tailless CD4 molecules can be endocytosed in lymphocytes, an inability to bind to the adaptors is unlikely to exclude CD4 from coated pits. The failure of CD4 to enter endocytic coated vesicles in lymphocytes is most easily explained by the interaction

of CD4 with another molecule or molecules. Comodulation and cross-linking experiments suggest that at least a portion of the CD4 on T cells may be associated with the TCR/CD3 complex (51–54). However, the TCR/CD3 complex is itself constitutively internalized and recycled on lymphocytes (55, 56), and is therefore unlikely to prevent CD4 endocytosis. Furthermore, MOLT-4 cells, which do not express cell surface TCR/CD3, show the same low levels of CD4 uptake observed on other T cell lines. The fact that cytoplasmic-deleted CD4 molecules were internalized equally efficiently when transfected into lymphocytic or HeLa cells suggests that the cytoplasmic domain of CD4 is involved in the exclusion of CD4 from coated pits in lymphocytes. As CD4 in lymphocytes is known to associate with the T cell specific tyrosine kinase p56<sup>lck</sup> (11, 12, 57, 58), it may be that p56<sup>lck</sup> directly or indirectly regulates CD4 endocytosis. Indeed, we have been able to immunoprecipitate kinase activity in association with CD4 from lysates of CEM, but not HeLa-CD4 or HL-60 cells, or the A2.01/CD4-cyt399 and A2.01/CD4-cyt401 cell lines (data not shown). Furthermore, transfection of the *lck* gene into NIH-3T3-CD4 cells specifically inhibited endocytosis of CD4 (A. Pelchen-Matthews, I. Boulet, R. Fagard, and M. Marsh, manuscript in preparation). The mechanism by which p56<sup>lck</sup> mediates this exclusion is at present unclear.

Collectively these data indicate that there are three distinct patterns of interaction between CD4 and cell surface coated pits, and that each pattern results in different rates of endocytosis and steady state levels of internalized CD4. First, CD4 alone, through its cytoplasmic domain, has a weak but definite interaction with the coated vesicle adaptors. This leads to relatively efficient endocytosis of the molecule in nonlymphoid cells, and significant levels of internalized CD4 (40%) at equilibrium. Deletion of the cytoplasmic domain reveals the second, default pathway; the truncated CD4 molecules follow the basal endocytic membrane trafficking in both transfected lymphocytes and nonlymphoid cells. The rate of uptake is reduced, and the equilibrium pool of internalized material is proportional to the ratio of the surface areas of the endosome and plasma membranes. Third, in lymphocytes, CD4 is largely excluded from coated pits, presumably by its interaction with the p56<sup>lck</sup> molecule, and only 5–10% of the CD4 is found intracellularly at equilibrium. These patterns of CD4 endocytosis suggest that plasma membrane proteins require specific signals either to direct their inclusion in coated pits and endocytosis (59), or to prevent their entry into coated pits. Molecules lacking both signals such as the tailless CD4, are neither included in nor excluded from coated pits and enter cells as components of the bulk membrane traffic. In agreement with this suggestion, low rates of endocytosis have been reported for other cytoplasmic-deleted molecules, including the immunoglobulin F<sub>c</sub> receptor II (60) and the transferrin receptor (61).

The observation that CD4 endocytosis in HL-60 cells closely

resembles that in transfected adherent tissue culture cells indicates that the different patterns of CD4 endocytosis may also occur in cells normally expressing CD4 and hence in vivo. While the function of CD4 on cells of the macrophage/monocyte lineage is not clear, CD4 on T cells binds MHC-II and, together with p56<sup>lck</sup>, appears to be directly involved in signal transduction. Although it is unclear how the T cell lines studied here relate to the different stages in T cell ontogeny in vivo, a role for CD4 internalization in T cell function can be proposed. T cell stimulation by phorbol esters, which mimics activation through protein kinase C, causes dissociation of CD4 and p56<sup>lck</sup> (62) and leads to CD4 endocytosis and downregulation (13–15). Similar effects may be induced during stimulation by anti-CD3 antibodies or by antigen. Binding experiments with T cell clones and artificial target cells bearing MHC-II have demonstrated that cell-cell adhesion is a dynamic process, with an adhesion phase followed by release (7). The release phase may be driven by the endocytic depletion of cell surface CD4, and render lymphocytes latent to additional activating signals.

In addition to its function in the immune system, CD4 is used as a receptor by HIV and may play multiple roles in AIDS. First, despite the extensive mapping of the interaction between the HIV surface glycoprotein gp120 and CD4, the subsequent events in virus entry which lead to fusion of the viral envelope with a cellular membrane (63) are unclear. HIV fusion is pH-independent (64, 65) and can potentially occur at the cell surface or within endosomes. HIV particles have been observed in endocytic vesicles and it has been argued that the endocytic pathway provides the primary route to productive infection (66). It is noteworthy that in all the CD4<sup>+</sup> cell lines we have studied, and with a number of CD4 mutants, we have observed some constitutive endocytosis of CD4. The levels of CD4 endocytosis were relatively high in the promyelocytic HL-60 cells, which may have relevance to the role of macrophages or monocytes as reservoirs for HIV (67). Furthermore, in the lymphocytic cell lines, where CD4 internalization is normally slow, the virus itself may stimulate CD4 uptake. Gp120 has been shown to cause CD4 phosphorylation (68), and may thereby induce p56<sup>lck</sup> dissociation, CD4 internalization, and T cell stimulation (69). Alternatively, crosslinking of CD4 through multivalent interactions with gp120 on the virus particle may also induce CD4 internalization. Second, in HIV-infected individuals, endocytic processes induced by the interaction of CD4 and gp120 may trigger the T cell anergy (70) that is proposed to contribute to the onset of AIDS.

A detailed knowledge of the control of CD4 levels at the cell surface and the pathways and regulation of CD4 endocytosis will thus be important in understanding the role of CD4 in T cell function. In addition, it may provide further insights into not only the processes involved in HIV infection and AIDS, but also the mechanisms of action of membrane-associated tyrosine kinases.

We thank Ruth Hollinshead, David Robertson, Catharine Clarke, and Rose Watson for help with the

electron microscopy, Dr. Peter Beverley for the 4120 antibody, Dr. Dan Littman for providing the A2.01/CD4-cyt399, A2.01/CD4-cyt401, and A3.01 cell lines, and Drs. Robin Weiss, John Moore, and Paul Quinn for critically reading the manuscript.

This work was supported by grants to the Institute of Cancer Research from the Cancer Research Campaign and the Medical Research Council.

Address correspondence to Mark Marsh, Chester Beatty Laboratories, Institute of Cancer Research, Fulham Road, London SW3 6JB, UK.

Received for publication 7 September 1990 and in revised form 3 December 1990.

## References

- Littman, D.R. 1987. The structure of the CD4 and CD8 genes. *Annu. Rev. Immunol.* 5:561.
- Parnes, J.R. 1989. Molecular biology and function of CD4 and CD8. *Adv. Immunol.* 44:265.
- Sattentau, Q.J., and R.A. Weiss. 1988. The CD4 antigen: physiological ligand and HIV receptor. *Cell.* 52:631.
- Stewart, S.J., J. Fujimoto, and R. Levy. 1986. Human T lymphocytes and monocytes bear the same Leu-3(T4) antigen. *J. Immunol.* 136:3773.
- Robey, E., and R. Axel. 1990. CD4: Collaborator in immune recognition and HIV infection. *Cell.* 60:697.
- Doyle, C., and J.L. Strominger. 1987. Interaction between CD4 and class II MHC molecules mediates cell adhesion. *Nature (Lond.)* 330:256.
- Rosenstein, Y., S.J. Burakoff, and S.H. Herrmann. 1990. HIV-gp120 can block CD4-class II MHC-mediated adhesion. *J. Immunol.* 144:526.
- Bank, I., and L. Chess. 1985. Perturbation of the T4 molecules transmits a negative signal in T cells. *J. Exp. Med.* 162:1294.
- Wassmer, P., C. Chan, L. Logdberg, and E.M. Shevach. 1985. Role of the L3T4 antigen in T cell activation. II. Inhibition of T cell activation by monoclonal anti-L3T4 antibodies in the absence of accessory cells. *J. Immunol.* 135:2237.
- Tite, J.P., A. Sloan, and J.A. Janeway. 1986. The role of L3T4 in T cell activation: L3T4 may be both an Ia-binding protein and a receptor that transduces a negative signal. *J. Mol. Cell. Immunol.* 2:179.
- Veillette, A., M.A. Bookman, E.M. Horak, and J.B. Bolen. 1988. The CD4 and CD8 T cell surface antigens are associated with the internal membrane tyrosine-protein kinase p56<sup>lck</sup>. *Cell.* 55:301.
- Rudd, C.E., J.M. Trevelyan, J.D. Dasgupta, L.L. Wong, and S.F. Schlossman. 1988. The CD4 receptor is complexed in detergent lysates to a protein-tyrosine kinase (pp58) from human T lymphocytes. *Proc. Natl. Acad. Sci. USA.* 85:5190.
- Acres, B.R., P.J. Conlon, D.Y. Mochizuki, and B. Gallis. 1986. Rapid phosphorylation and modulation of the T4 antigen on cloned helper T cells induced by phorbol myristate acetate or antigen. *J. Biol. Chem.* 34:16210.
- Hoxie, J.A., D.M. Matthews, K.J. Callahan, D.L. Cassel, and R.A. Cooper. 1986. Transient modulation and internalization of T4 antigen induced by phorbol esters. *J. Immunol.* 137:1194.
- Hoxie, J.A., J.L. Rackowski, B.S. Haggarty, and G.N. Gaulton. 1988. T4 Endocytosis and phosphorylation induced by phorbol esters but not by mitogen or HIV infection. *J. Immunol.* 140:786.
- Pelchen-Matthews, A., J.E. Armes, and M. Marsh. 1989. Internalization and recycling of CD4 transfected into HeLa and NIH3T3 cells. *EMBO (Eur. Mol. Biol. Organ.) J.* 8:3641.
- Marsh, M., J.E. Armes, and A. Pelchen-Matthews. 1990. Endocytosis and recycling of CD4. *Biochem. Soc. Trans.* 18:139.
- Slot, J.W., and H.J. Geuze. 1985. A novel method to make gold probes for multiple labeling cytochemistry. *Eur. J. Cell Biol.* 38:87.
- Maddon, P.J., A.G. Dalgleish, J.S. McDougal, P.R. Clapham, R.A. Weiss, and R. Axel. 1986. The T4 gene encodes the AIDS virus receptor and is expressed in the immune system and the brain. *Cell.* 47:333.
- Maddon, P.J., J.S. McDougal, P.R. Clapham, A.G. Dalgleish, S. Jamal, R.A. Weiss, and R. Axel. 1988. HIV infection does not require endocytosis of its receptor, CD4. *Cell.* 54:865.
- Smith, S.D., M. Shatsky, P.S. Cohen, R. Warnke, M.P. Link, and B.E. Glader. 1984. Monoclonal antibody and enzymatic profiles of human malignant T-lymphoid cells and derived cell lines. *Cancer Res.* 44:5657.
- Foley, G.E., H. Lazarus, S. Farber, B.G. Uzman, B.A. Boone, and R.E. McCarthy. 1965. Continuous culture of human lymphoblasts from peripheral blood of a child with acute leukemia. *Cancer (Phila.)* 18:522.
- Bedinger, P., A. Moriarty, R.C. von Borstel II, N.J. Donovan, K.S. Steimer, and D.R. Littman. 1988. Internalization of the human immunodeficiency virus does not require the cytoplasmic domain of CD4. *Nature (Lond.)* 334:162.
- Collins, S.J., R.C. Gallo, and R.E. Gallagher. 1977. Continuous growth and differentiation of human myeloid leukemic cells in suspension culture. *Nature (Lond.)* 270:347.
- Deen, K.C., J.S. McDougal, R. Inacker, G. Folena-Wasserman, J. Arthos, J. Rosenberg, P.J. Maddon, R. Axel, and R.W. Sweet. 1988. A soluble form of CD4 (T4) protein inhibits AIDS virus infection. *Nature (Lond.)* 331:82.
- Armes, J.E. 1990. The cell biology of the human immunodeficiency virus receptor, CD4. PhD thesis. University of London, London. pp. 1-264.
- Griffiths, G., R. Back, and M. Marsh. 1989. A quantitative analysis of the endocytic pathway in baby hamster kidney cells. *J. Cell Biol.* 109:2703.
- Marsh, M., S. Schmid, H. Kern, E. Harms, P. Male, I. Mellman, and A. Helenius. 1987. Rapid analytical and preparative isolation of functional endosomes by free flow electrophoresis. *J. Cell Biol.* 104:875.
- Smith, P.K., R.I. Krohn, G.T. Hermanson, A.K. Mallia, F.H. Gartner, M.D. Provenzano, E.K. Fujimoto, N.M. Goeke, B.J. Olson, and D.C. Klenk. 1985. Measurement of protein using bicinchoninic acid. *Anal. Biochem.* 150:76.
- Helenius, A., J. Kartenbeck, K. Simons, and E. Fries. 1980. On the entry of Semliki Forest virus into BHK-21 cells. *J. Cell*

- Biol.* 84:404.
31. Weibel, E.R. 1979. *Stereological Methods. I. Practical methods for biological morphometry.* Academic Press Inc., New York.
  32. Gundersen, H.J.G., and E.B. Jensen. 1985. Stereological estimation of the volume-weighted mean volume of arbitrary particles observed on random sections. *J. Microsc. (Oxf.)* 138:127.
  33. Griffiths, G., S.D. Fuller, R. Back, M. Hollinshead, S. Pfeiffer, and K. Simons. 1989. The dynamic nature of the Golgi complex. *J. Cell Biol.* 108:277.
  34. Aherne, W.A., and M.S. Dunnill. 1982. *Morphometry.* Edward Arnold, London. pp. 1-220.
  35. Rao, P.E., M.A. Talle, P.C. Kung, and G. Goldstein. 1983. Five epitopes of a differentiation antigen on human inducer T cells distinguished by monoclonal antibodies. *Cell. Immunol.* 80:310.
  36. Richardson, N.E., N.R. Brown, R.E. Hussey, A. Vaid, T.J. Matthews, D.P. Bolognesi, and E.L. Reinherz. 1988. Binding site for human immunodeficiency virus coat protein gp120 is located in the NH<sub>2</sub>-terminal region of T4 (CD4) and requires the intact variable-region-like domain. *Proc. Natl. Acad. Sci. USA.* 85:6102.
  37. Anderson, R.G.W., M.S. Brown, and J.L. Goldstein. 1977. Role of the coated endocytic vesicle in the uptake of receptor-bound low density lipoprotein in human fibroblasts. *Cell.* 10:351.
  38. Marsh, M., and A. Helenius. 1980. Adsorptive endocytosis of Semliki Forest virus. *J. Mol. Biol.* 142:439.
  39. Steinman, R.M., S.E. Brodie, and Z.A. Cohn. 1976. Membrane flow during pinocytosis. A stereologic analysis. *J. Cell Biol.* 68:665.
  40. Besterman, J.M., J.A. Airhart, R.C. Woodworth, and R.B. Low. 1981. Exocytosis of pinocytosed fluid in cultured cells: kinetic evidence for rapid turnover and compartmentation. *J. Cell Biol.* 91:716.
  41. Swanson, J.A., B.D. Yirinec, and S.C. Silverstein. 1985. Phorbol esters and horseradish peroxidase stimulate pinocytosis and redirect the flow of pinocytosed fluid in macrophages. *J. Cell Biol.* 100:851.
  42. Kletzien, R.F., M.W. Pariza, J.E. Becker, and V.R. Potter. 1975. A method using 3-O-methyl-D-glucose and phloretin for the determination of intracellular water space of cells in monolayer culture. *Anal. Biochem.* 68:537.
  43. Carpentier, J.-L., E. van Obberghen, P. Gorden, and L.C. Orci. 1981. Surface redistribution of <sup>125</sup>I-Insulin in cultured human lymphocytes. *J. Cell Biol.* 91:17.
  44. Griffiths, G., R. Matteoni, R. Back, and B. Hoflack. 1990. Characterization of the cation independent mannose-6-phosphate receptor-enriched pre-lysosomal compartment in NRK cells. *J. Cell Sci.* 95:441.
  45. Parton, R.G., K. Prydz, M. Bomsel, K. Simons, and G. Griffiths. 1989. Meeting of the apical and basolateral endocytic pathways of the Madin-Darby canine kidney cell in late endosomes. *J. Cell Biol.* 109:3259.
  46. Maddon, P.J., D.R. Littman, M. Godfrey, D.E. Maddon, L. Chess, and R. Axel. 1985. The isolation and nucleotide sequence of a cDNA encoding the T cell surface protein T4: A new member of the immunoglobulin gene family. *Cell.* 42:93.
  47. Folks, T., D.M. Powell, M.M. Lightfoote, S. Benn, M.A. Martin, and A.S. Fauci. 1986. Induction of HTLV-III/LAV from a nonvirus-producing T-cell line: Implications for latency. *Science (Wash. DC).* 231:600.
  48. Goldstein, J.L., M.S. Brown, R.G.W. Anderson, D.W. Russell, and W.J. Schneider. 1985. Receptor-mediated endocytosis: Concepts emerging from the LDL receptor system. *Annu. Rev. Cell Biol.* 1:1.
  49. Bleil, J.D., and M.S. Bretscher. 1982. Transferrin receptor and its recycling in HeLa cells. *EMBO (Eur. Mol. Biol. Organ.) J.* 1:351.
  50. Pearse, B.M.F., and M.S. Robinson. 1990. Clathrin adaptors and sorting. *Annu. Rev. Cell Biol.* 6: In press.
  51. Anderson, P., M.-L. Blue, and S.F. Schlossman. 1988. Evidence for a specific association between CD4 and approximately 5% of the CD3/T cell receptor complexes in helper T lymphocytes. *J. Immunol.* 140:1732.
  52. Emmrich, F., L. Kanz, and K. Eichmann. 1987. Cross-linking of the T cell receptor complex with the subset-specific differentiation antigen stimulates interleukin 2 receptor expression in human CD4 and CD8 T cells. *Eur. J. Immunol.* 17:529.
  53. Ledbetter, J.A., C.H. June, P.S. Rabinovitch, A. Grossman, T.T. Tsu, and J.B. Imboden. 1988. Signal transduction through CD4 receptors: Stimulatory vs. inhibitory activity is regulated by CD4 proximity to the CD3/T cell receptor. *Eur. J. Immunol.* 18:525.
  54. Saizawa, K., J. Rojo, and C.A. Janeway. 1987. Evidence for a physical association of CD4 and the CD3:α:β T-cell receptor. *Nature (Lond.)* 328:260.
  55. Krangel, M.S. 1987. Endocytosis and recycling of the T3-T cell receptor complex. *J. Exp. Med.* 165:1141.
  56. Minami, Y., L.E. Samelson, and R.D. Klausner. 1987. Internalization and cycling of the T cell antigen receptor. Role of protein kinase C. *J. Biol. Chem.* 262:13342.
  57. Shaw, A.S., K.E. Amrein, C. Hammond, D.F. Stern, B.M. Sefton, and J.K. Rose. 1989. The *lck* tyrosine protein kinase interacts with the cytoplasmic tail of the CD4 glycoprotein through its unique amino-terminal domain. *Cell.* 59:627.
  58. Turner, J.M., M.H. Brodsky, B.A. Irving, S.D. Levin, R.M. Perlmutter, and D.R. Littman. 1990. Interaction of the unique N-terminal region of tyrosine kinase p56<sup>lck</sup> with cytoplasmic domains of CD4 and CD8 is mediated by cysteine motifs. *Cell.* 60:755.
  59. Bretscher, M.S., J.N. Thomson, and B.M.F. Pearse. 1980. Coated pits act as molecular filters. *Proc. Natl. Acad. Sci. USA.* 77:4156.
  60. Miettinen, H.M., J.K. Rose, and I. Mellman. 1989. Fc receptor isoforms exhibit distinct abilities for coated pit localization as a result of cytoplasmic domain heterogeneity. *Cell.* 58:317.
  61. Jing, S., T. Spencer, K. Miller, C. Hopkins, and I.S. Trowbridge. 1990. Role of the human transferrin receptor cytoplasmic domain in endocytosis: Localization of a specific signal sequence for internalization. *J. Cell Biol.* 110:283.
  62. Hurley, T.R., K. Luo, and B.M. Sefton. 1989. Activators of protein kinase C induce dissociation of CD4, but not CD8, from p56<sup>lck</sup>. *Science (Wash. DC).* 245:407.
  63. Marsh, M., and A. Helenius. 1989. Virus entry into animal cells. *Adv. Virus Res.* 36:107.
  64. Stein, B.S., S.D. Gowda, J.D. Lifson, R.C. Penhallow, K.G. Bensch, and E.G. Engleman. 1987. pH-Independent HIV entry into CD4-positive T cells via virus envelope fusion to the plasma membrane. *Cell.* 49:659.
  65. McClure, M.O., M. Marsh, and R.A. Weiss. 1988. Human immunodeficiency virus infection of CD4-bearing cells occurs by a pH-independent mechanism. *EMBO (Eur. Mol. Biol. Organ.) J.* 7:513.
  66. Pauza, C.D., and T.M. Price. 1988. Human immunodeficiency virus infection of T cells and monocytes proceeds via receptor-mediated endocytosis. *J. Cell Biol.* 107:959.

67. Gendelman, H.E., J.M. Orenstein, M.A. Martin, C. Ferrua, R. Mitra, T. Phipps, L.A. Wahl, H.C. Lane, A.S. Fauci, D.S. Burke, D. Skillman, and M.S. Meltzer. 1988. Efficient isolation and propagation of human immunodeficiency virus on recombinant colony-stimulating factor 1-treated monocytes. *J. Exp. Med.* 167:1428.
68. Fields, A.P., D.P. Bednarik, A. Hess, and W.S. May. 1988. Human immunodeficiency virus induces phosphorylation of its cell surface receptor. *Nature (Lond.)* 333:278.
69. Kornfeld, H., W.W. Cruikshank, S.W. Pyle, J.S. Berman, and D.M. Center. 1988. Lymphocyte activation by HIV-1 envelope glycoprotein. *Nature (Lond.)* 335:445.
70. Mittler, R.S., and M.K. Hoffman. 1989. Synergism between HIV gp120 and gp120-specific antibody in blocking human T cell activation. *Science (Wash. DC)* 245:1380.